Author/s:
Verma, S;Shakya, VPS;Idnurm, A

Title:
The dual function gene RAD23 contributes to Cryptococcus neoformans virulence independently of its role in nucleotide excision DNA repair

Date:
2019-10-30

Citation:
Verma, S., Shakya, V. P. S. & Idnurm, A. (2019). The dual function gene RAD23 contributes to Cryptococcus neoformans virulence independently of its role in nucleotide excision DNA repair. Gene, 717, https://doi.org/10.1016/j.gene.2019.144043.

Persistent Link:
https://hdl.handle.net/11343/301561

The dual function gene *RAD23* contributes to *Cryptococcus neoformans* virulence independently of its role in nucleotide excision DNA repair

Surbhi Verma[a,b], Viplendra P. S. Shakya[a,b] and Alexander Idnurm[a,c]*

[a] *Division of Cell Biology and Biophysics, School of Biological Sciences, University of Missouri-Kansas City, Kansas City, Missouri, USA*

[b] *Department of Biochemistry, University of Utah School of Medicine, Salt Lake City, Utah, USA*

[c] *School of BioSciences, University of Melbourne, Parkville, VIC, Australia*

* Correspondence: alexander.idnurm@unimelb.edu.au

Abstract

Genes involved in the repair of DNA damage are emerging as playing important roles during the disease processes caused by pathogenic fungi. However, there are potentially hundreds of genes involved in DNA repair in a fungus and some of those genes can play additional roles within the cell. One such gene is *RAD23*, required for virulence of the human pathogenic fungus *Cryptococcus neoformans*, that encodes a protein involved in the nucleotide excision repair (NER) pathway. However, Rad23 is a dual function protein, with a role in either repair of damaged DNA or protein turn over by directing proteins to the proteasome. Here, these two functions of Rad23 were tested by the creation of a series of domain deletion alleles of *RAD23* and the assessment of the strains for DNA repair, proteasome functions, and virulence properties. Deletion of the different domains was able to uncouple the two functions of Rad23, and the phenotypes of strains carrying such forms indicated that the role of *RAD23* in virulence is due to its function in proteasomal-mediated protein degradation rather than NER.

Keywords: protein domain, proteasome, site-directed mutagenesis, tunicamycin, ubiquitin-binding, ultraviolet

1. Introduction

Cryptococcus neoformans is an opportunistic fungal pathogen and, like many other pathogens, it has to survive in the environment, and then establish and adapt in its host to be able to cause disease. Different cellular signaling pathways and processes have been studied in the context of fitness in the environment and host (Bahn and Jung, 2013), to reveal important insights. For instance, DNA repair genes have essential roles in maintaining genomic integrity and they play key roles in environmental survival, evolution and pathogenicity (Billmyre et al., 2017; Boyce et al., 2017; Jung et al., 2019; Jung et al., 2016; Palmer et al., 2018; Verma and Idnurm, 2013). Along with the integrity of the pathogen's DNA, another important aspect that relates to the survival and pathogenicity is the proper maintenance of a cell's protein composition. Different genes related to the endoplasmic-reticulum-associated protein degradation (ERAD) pathway, the unfolded protein response (UPR) (Cheon et al., 2014) and ubiquitin proteasome system also have roles in fungal virulence (Liu and Xue, 2011; Liu and Xue, 2014).

The *RAD23* gene is implicated in the virulence of *C. neoformans*. In a large scale study of gene functions in *C. neoformans*, 1,200 of the 7,000 genes in the genome were deleted and the knockout strains tested for three "classical" virulence traits, which are growth at 37°C, capsule formation and melanization, and competitive survival between mixed populations of strains in a mouse model of disease as a measure of virulence (Liu et al., 2008). The *rad23* mutant was ranked 57th for reduced virulence, yet had no impairments in known virulence traits.

Rad23 is a component of the nucleotide excision repair (NER) pathway that was first identified through the isolation of UV sensitive mutants in the model yeast *Saccharomyces cerevisiae* (McKnight et al., 1981). Positional cloning and then sequencing of the *RAD23* gene revealed the surprising feature that parts of the predicted protein have similarity to ubiquitin (Watkins et al., 1993). Rad23 is hence a dual function protein with one role in DNA repair and the second as a ubiquitin receptor involved in the proteasomal degradation pathway (Dantuma et al., 2009). From *S. cerevisiae* to humans, Rad23 is part of NER through its interactions with another NER protein, Rad4 (XPC in humans) (Guzder et al., 1998). The Rad23 contribution to both DNA repair and proteasomal degradation is also conserved in plants (Farmer et al., 2010; Lahari et al., 2017). The role of Rad4 in DNA repair is to recognize and bind to UV-induced photolesions (Min and Pavletich, 2007).

The Rad23 protein has four defined domains that are conserved from the model fungus *S. cerevisiae* to humans (Dantuma et al., 2009; Walters et al., 2003). These four domains are abbreviated as UBL, UBA1, Rad4 or XPC-binding (XPCB) and UBA2, and each domain has a specific function. The domains of Rad23 are best characterized in *S. cerevisiae* (Dantuma et al., 2009) and relate to either DNA repair (via NER) or the proteasome-mediated degradation of unwanted proteins. The N-terminal domain UBL is ubiquitin-like and it binds to the Rpn1 subunit of the 19S regulatory subunit of the proteasome (Elsasser et al., 2002). Other proteins that bind to the UBL domain of Rad23 are the ubiquitin chain elongation factor Ufd2 (Kim et al., 2004), peptidyl tRNA hydrolase Pth2 (Ishii et al., 2006) and ubiquitin associated domains (UBA) within Rad23 itself (Walters et al., 2003). The central UBA1 domain binds to ubiquitin/polyubiquitin molecules and UBL, and the C-terminal UBA2 domain binds to ubiquitin and the UBL domain.

The intra-protein interaction of UBL and UBA domains prevents continuous binding of Rad23 to the proteasome, as the protein adopts a closed conformation. UBA domains are so named because they are able to bind ubiquitin and polyubiquitin molecules. The human Rad23 A and B isoforms use their C-terminal UBA2 domains to bind to base excision DNA repair protein 3-methyladenine DNA glycosylase (MPG) (Miao et al., 2000), and the UBA2 domain is sufficient for this binding (Yokoi and Hanaoka, 2017). Either of the two human Rad23 proteins can increase binding of MPG to its DNA damage substrate and stimulate its DNA glycosylase activity. The UBA2 domain of Rad23 A protein binds to human immunodeficiency (HIV) 1 accessory protein Vpr (Withers-Ward et al., 2000). The UBA2 domain is required for the stability of the Rad23 protein in its interaction with the proteasome. The UBA2 domain resists initiation of degradation by the proteasome and hence can efficiently channel a substrate for degradation while preventing its own degradation (Heinen et al., 2011). The third domain of Rad23 is the Rad4-binding domain, also called the XPCB domain in humans, and this domain is important for the NER activity of the Rad23 protein. This domain interacts with Rad4 and the peptide *N*-glycanase protein Png1 (Lee et al., 2005) and primarily contributes to the DNA repair function associated with Rad23.

Another important function of *RAD23* is its global impact on transcription. For instance, in *S. cerevisiae RAD23* is involved in the regulation of almost two-thirds of the UV-regulated genes, and almost one third of all yeast genes are mis-regulated in a *rad23* knockout strain (Wade and Auble, 2010; Wade et al., 2009). As a consequence, Rad23 is involved in cell cycle regulation and phosphate metabolism. These functions may relate to proteasome-mediated degradation or NER.

The multiple functions of Rad23 raise the question about which relate to the virulence of *C. neoformans*. Hence, in this study we aimed to uncouple the role of the two major different functions of *RAD23*, DNA repair and protein sorting, by creating alleles of the gene impaired in each property, and then testing the virulence and other phenotypes of strains carrying them.

2. Materials and Methods

2.1. Generation of RAD23 knockout, RAD23 full length and domain deletion complementation constructs and strains

The fungal strains used is this study are listed in table 1. For generation of a *RAD23* knockout the *RAD23*::*NAT* cassette was amplified from the genomic DNA of the previously generated *rad23* gene disruption strain (Liu et al., 2008) using primer set AISV49 and AISV50. The knockout cassette was transformed by biolistics with the Bio-Rad particle delivery system into the KN99**a** strain background, and transformants were selected on YPD medium + nourseothricin (100 µg/ml). Gene replacement in the *rad23*Δ strain was confirmed by PCR and Southern blotting. This new gene replacement strain was constructed because the parent strain used to create the original *rad23*Δ mutant has accumulated background mutations during in vitro passage such that it is less pathogenic and fertile than other versions (Arras et al., 2017; Janbon et al., 2014).

To complement the *rad23*Δ strain, full length *RAD23* with its native promoter and terminator was amplified from genomic DNA of strain KN99α using primers AISV118/AISV119. The amplified PCR product was cloned in the pCR2.1 TOPO-TA vector and transformed by heat shock into *Escherichia coli* strain DH5α cells. The plasmids isolated were sequenced to identify one with the

137 correct sequence of *RAD23*. The RAD23 gene was excised from the TA vector using BamHI
138 restriction enzyme, and plasmid pPZP-NEO11 was digested with BamHI. The two digestion
139 products were ligated and the resulting product p*PZP*-Pnative-*RAD23*-T-*NEO* was transformed
140 into *E. coli*. The clones were further verified by PCR of the resulting plasmids and by sequencing.
141 The error-free version of p*PZP*-Pnative-*RAD23*-T-*NEO* was transformed by electroporation into
142 *Agrobacterium tumefaciens* strain EHA105. The *A. tumefaciens* strain containing p*PZP*-Pnative-
143 *RAD23*-T-*NEO* was then co-cultured with the *C. neoformans rad23*Δ strain for delivery of the T-
144 DNA. Fungal transformants were selected for growth on YPD + G-418 (100 µg/ml) + cefotaxime
145 (200 µg/ml) plates, and integration of the T-DNA into the genome was verified by PCR.
146
147 To generate of *RAD23* individual domain deletion constructs, the p*PZP*-Pnative-*RAD23*-T-*NEO*
148 construct was used as a template for site-directed mutagenesis. Primers were designed specific for
149 each type of domain deletion (Table S1). For performing the domain deletions, the QuickChange
150 II XL Site-Directed Mutagenesis Kit (Agilent Technologies, Foster City, CA) was used following
151 the manufacturer's protocol, with the extension temperature of 68°C for 15 min for 18 cycles.
152 After DpnI digestion, the treated mix was transformed by heat shock into *E. coli* DH5α cells. The
153 plasmids obtained from the transformants were verified by sequencing, for all four-domain
154 deletions (*RAD23-ubl*Δ, *RAD23-uba1*Δ, *RAD23-xpcb*Δ and *RAD23-uba2*Δ). For generating the
155 double domain deletion constructs *RAD23-ubl*Δ+*uba1*Δ and *RAD23-uba1*Δ+*uba2*Δ, a second
156 round of site-directed mutagenesis was employed. The template constructs used were pPZP-NEO-
157 *RAD23-ubl*Δ and pPZP-NEO-*RAD23-uba2*Δ, with the primer set AISV142/AISV143 used to
158 delete the UBA1 domain. The protocol followed was the same as for the single domain deletion
159 strains. Plasmids confirmed by sequencing analysis to be error free were then transformed into *A.*

tumefaciens, used to deliver the T-DNA with the *RAD23* alleles into the *rad23*Δ strain to obtain *C. neoformans* strains carrying new alleles of *RAD23*. A list of plasmids is included as Table S2.

2.2. Rad23 subcellular localization

A *RAD23-GFP* fusion construct was made. Strain KN99α genomic DNA was used as the template to amplify the *RAD23* gene using primers AISV165/AISV166 with a NcoI site in both the primers. The p*PZP-HXK2-GFP-NAT* vector was also digested with NcoI. The NcoI-digested *RAD23* amplicon and NcoI-digested p*PZP-GFP-NAT* vector (without the *HXK2* insert) were ligated with T4 DNA ligase and transformed into *E. coli*. The cloning strategy places a *RAD23-GFP* fusion under control of the constitutive histone H3 promoter when transformed into *C. neoformans* cells. The recombinant p*PZP-RAD23-GFP-NAT* construct was sequenced for the *RAD23-GFP* fusion and a correct construct was then transformed into *A. tumefaciens*. The transformed *A. tumefaciens* strain was co-cultured with KN99**a**. Positive transformants were selected for growth on YPD + nourseothricin + cefotaxime plates. The strains were scanned for green fluorescence. Using the same construct within the *rad23*Δ strain was not possible because it confers resistance to nourseothricin. *NAT* was therefore switched with *NEO* as a selectable marker in the pPZP- *RAD23-GFP-NAT* construct. For this switch, pPZP-*RAD23-GFP-NAT* was digested with EcoRI to remove the *NAT* fragment, and into the empty EcoRI site was inserted an EcoRI-digested *NEO* fragment from plasmid pPZP-NEO11. Ligated pPZP-*RAD23-GFP-NEO* was transformed into *E. coli* DH5α, and then the correct plasmid was transformed into *A. tumefaciens* EHA105. This *A. tumefaciens* strain was co-cultured with the *rad23*Δ strain. Transformants were selected for growth on YPD + G-418 + cefotaxime plates. The strains expressing *RAD23-GFP* were grown to logarithmic phase in liquid YPD media, stained with nuclear stain DAPI (1 μg/ml) and

mitochondrial stain MitoTracker Red CMXRos (3 nM; Invitrogen, Carlsbad, CA). Cells were incubated in dark for 20 min, washed and resuspended in phosphate buffered saline (PBS) and were examined by fluorescence microscopy.

To make the domain deletion GFP constructs for *RAD23-uba2*Δ, the p*PZP-RAD23*-GFP-*NEO* construct was used as the template and the primer combination AISV146/AISV147, with the QuickChange II XL Site–Directed Mutagenesis Kit as described above. The constructs obtained were sequenced, an error-free version identified and used for *Agrobacterium*-mediated transformation into the *rad23*Δ strain. The *rad23*Δ+*RAD23-uba2*Δ-GFP strain was used for fluorescence microscopy as described above.

2.3. Stress assays for the C. neoformans strains

C. neoformans strains were exposed to different kinds of stress. Strains were grown overnight in liquid YPD medium at 30°C. The strains were serially diluted, 10-fold each time, up to 10^{-6} dilution, then spotted on a YPD medium plate as the control or on YPD + stressor. Strains were checked for growth at 37°C. For endoplasmic reticulum stress tunicamycin (0.125 μg/ml) or dithiothreitol (DTT; 10 mM) were used, for DNA damage or oxidative stress *tert*-butyl-hydroperoxide (t-BOOH; 0.3 mM or 0.6 mM), hydrogen peroxide (H_2O_2; 1 mM) or Paraquat (0.5 mM) were used. The UV sensitivities of strains were tested by applying UV (120 J/m^2) in an XL-1500 UV cross linker (Spectronics Corporation, Lincoln, NE). The unstressed control and stress plates were incubated at 30°C for 2 days.

2.4. Virulence assays in wax moth larvae

The *Galleria mellonella* (wax moth) assay of the virulence of *C. neoformans* strains followed methods previously described (Mylonakis et al., 2005). Overnight cultures in YPD medium were washed three times with PBS. Cells were suspended in PBS to 2×10^7 cells/ml. For each strain sets of 10-11 larvae were injected with 5 µl of the cells, as well as the control PBS. Wax moth were incubated at 37°C and survival monitored daily. Wild type KN99**a**, *rad23*Δ, the *rad23*Δ+*RAD23* complementation strain and the six domain deletion strains *rad23*Δ+*RAD23-ubl*Δ, *rad23*Δ+*RAD23-uba1*Δ, *rad23*Δ+*RAD23-xpcb*Δ, *rad23*Δ+*RAD23-uba2*Δ, *rad23*Δ+*RAD23-ubl*Δ+*uba1*Δ and *rad23*Δ+*RAD23-uba1*Δ+*uba2*Δ were inoculated. For this experiment, two independent transformants carrying the *RAD23* alleles were inoculated into the larvae, to eliminate the unlikely chance of the T-DNA inserting accidentally into genes that would be required for virulence.

3. Results

3.1. Mutation of RAD23 causes stress response phenotypes in C. neoformans

The *RAD23* gene was deleted in the wild type KN99**a** background of *C. neoformans* to yield a *rad23*Δ strain. The full-length *RAD23* gene was transformed into the *rad23*Δ strain to confirm that it restored any phenotypes back to the wild type level. Three strains, wild type, *rad23*Δ and complementation *rad23*Δ+*RAD23*, were tested for their phenotypes related to UV stress response (Fig. 1A). These strains were also tested for growth at 37°C and in the presence of tunicamycin, which disrupts the ERAD pathway and hence triggers ER stress (Fig. 1B). The *rad23*Δ strain has increased sensitivity to UV stress compared to wild type parent strain, consistent with the role of

Rad23 in NER. Also, *rad23*Δ shows increased resistance to tunicamycin, an indication of its role in ERAD or UPR (unfolded protein response). The complementation of *rad23*Δ with full length *RAD23* rescued the UV sensitivity and tunicamycin resistance phenotypes (Fig. 1A and 1B). In contrast, there was no growth defect at 37°C or to oxidative stress agents, hydrogen peroxide and Paraquat, in the *rad23*Δ strain (Fig. 1B).

3.2. Different parts of Rad23 impact the stress sensitivity

Rad23 has four domains - UBL, UBA1, XPCB and UBA2 - with each domain having a specific function. Though these individual domain functions of Rad23 have been dissected in *S. cerevisiae* (Dantuma et al., 2009), their functions are yet to be established in *C. neoformans*. To uncouple the role of DNA repair versus ubiquitin receptor function of Rad23 in *C. neoformans*, we deleted all four domains one at a time and in two combinational double domain deletions. In *S. cerevisiae* either UBA1 and UBA2 deletion singly or in combination does not affect UV sensitivity (Bertolaet et al., 2001). Hence, we created alleles with the equivalent types of deletions, as with different domain deletions it is possible to compare the function of individual domains with the full-length protein in *C. neoformans*. The plasmid used to complement the *rad23*Δ strain, that is *RAD23* with its native promoter and terminator, was used as the basis to make subsequent domain deletion constructs by site-directed mutagenesis. These constructs were transformed into the *rad23*Δ strain to create six resultant strains: *rad23*Δ+*RAD23-ubl*Δ (UBL domain deletion), *rad23*Δ+*RAD23-uba1*Δ (UBA1 domain deletion), *rad23*Δ+*RAD23-xpcb*Δ (XPCB domain deletion), *rad23*Δ+*RAD23-uba2*Δ (UBA2 domain deletion), *rad23*Δ+*RAD23-ubl*Δ+*uba1*Δ (UBL+UBA1 double domain deletion) and *rad23*Δ+*RAD23-uba1*Δ+*uba2*Δ (UBA1+UBA2 double domain deletion), as illustrated in Fig. 2.

The strains were compared under different stresses, i.e. UV light and *t*-butyl hydroperoxide (T-BOOH) to explore the role of the Rad23 domains under DNA damage stress conditions and tunicamycin and dithiothreitol (DTT) for their role in the UPR (Fig. 2). The XPCB domain deletion and UBA2 domain deletion strains showed different levels of sensitivity to UV stress, with the XPCB domain deletion strain being more sensitive, and comparable to the *rad23*Δ strain (Fig. 2). The UBA2 domain deletion strain exhibited a slight increase in UV sensitivity. Deletion of XPCB and UBA2 domains individually caused increased resistance to tunicamycin, like *rad23*Δ. The UBA2 domain deletion strain was more resistant compared to the XPCB domain deletion strain when strains were compared for growth a day after the stress. As the UBL and UBA1 domain individual domain deletion strains showed a wild type phenotype, these domains are not required to combat any of the tested stresses, at least individually. The strain with the double deletion of both domains UBL and UBA1 was also tested to see if there is any difference in stress tolerance compared to the individual domain deletions. No difference in tolerance to stresses was observed for the UBL+UBA1 double domain deletion strain, as it was comparable to the wild type strain (Fig. 2). For DTT and T-BOOH no phenotypic difference was observed for any of the domain deletion strains. For DTT stress one expectation was that the UBA2 domain and XPCB domain deletion strains would show similar phenotypes as observed in response to tunicamycin, since both chemicals can trigger the UPR. However, the absence of a phenotype in DTT treated XPCB domain and UBA2 domain deletion strains suggests a role of Rad23 at different levels in UPR, since DTT and tunicamycin trigger the UPR in different ways. Tunicamycin affects the *N*-linked glycosylation of proteins and DTT is a strong reducing agent, particularly of disulfide bonds. Since the UBA1 domain and UBA2 domain are both UBA domains, a strain missing both UBA1+UBA2

277 domains was generated to see if there is any additive effect in the phenotype. To our surprise, the
278 deletion of both these domains in combination resulted in a strain that was slightly more resistant
279 to tunicamycin compared to the individual UBA2 domain deletion strain. No additive effect was
280 observed for the UV sensitivity phenotype.
281
282 To summarize, the phenotypes exhibited by the strains with different alleles of *RAD23* indicate
283 that the XPCB domain of Rad23 is mainly responsible for the UV sensitive phenotype observed
284 for *rad23*Δ, and both XPCB and UBA2 domains for the tunicamycin resistance phenotype. Also,
285 when both UBA domains are removed together from Rad23 there should be increased impairment
286 of the ubiquitin receptor function that is not observed for the individual UBA1 domain deletion.
287
288 *3.3. Individual Rad23 domains have differing impact on the virulence of C. neoformans*
289 The impact of removing different domains in Rad23 on virulence was analyzed using the wax
290 moth (*Galleria mellonella*) larvae model of disease, which is an established alternative host to
291 mice, especially for testing many fungal strains. The percentage survival curves for larvae infected
292 with wild type, *rad23*Δ, *rad23*Δ+*RAD23* and individual and combinational domain deletion strains
293 are shown in Fig. 3. The data show the lowest survival for larvae infected with the wild type,
294 complemented (*rad23*Δ+*RAD23*) and XPCB domain deletion strains, where almost 90 percent of
295 the wax moth died by day 6 to day 7 post-inoculation. Also, the percentage survival is less for the
296 wax moth infected with strains with the UBL domain deletion, UBA1 domain deletion and
297 UBA1+UBL domain deletion (data not shown). For the *rad23*Δ and UBA2 domain deletion
298 strains, larval survival is highest, with close to 95 % still alive at five days post-inoculation and
299 almost 65 % at six days post-inoculation. A similar pattern occurred for the UBA1+UBA2 deletion

strains with 95 % and 57 % larval survival at day 5 and day 6, respectively. However, for the UBA1+UBA2 domain deletion strain towards day 7 there is a sudden fall in wax moth survival reaching 20 to 25 % survival by day 7, but then tapers and the remaining infected wax moth are alive until day 11 to 12, which is comparable to the *rad23*Δ and the UBA2 domain deletion strains. Statistical analysis of these survival data using the log-rank (Mantel-Cox) test indicated that there were significant differences with *rad23*Δ, UBA2 domain deletion and UBA1+UBA2 domain deletion strains versus the wild type strain with P-values of 0.0023, 0.0085, 0.0243, respectively. For all other individual and combinatorial domain deletion strains, UBL, UBA1, XPCB, UBL+UBA1 and for the *RAD23* complemented strain *rad23*Δ+*RAD23* the differences in larval survival were non-significant (P-values > 0.05).

3.4. Organelle localization and expression of Rad23-GFP and Rad23-DIVΔ-GFP

Rad23 is a DNA repair protein and an ubiquitin receptor whose localization could be in different subcellular compartments. The bioinformatics localization of Rad23 using PSORT II (Nakai and Kanehisa, 1992) predicted the protein to be 34.8 % nuclear, 34.8 % mitochondrial, 17.4 % cytoplasmic, and the rest from vesicle secretory system and vacuolar. To determine the subcellular localization of full length *RAD23*, GFP was fused to the C-terminal end of Rad23. The *RAD23*-GFP expressing strain was stained with nuclear stain DAPI and mitochondrial stain MitoTracker separately, and examined by fluorescence microscopy. *RAD23*-GFP clearly co-localized with nuclear stain DAPI, and hence Rad23 is partially nuclear (Fig. 4B). However, the Rad23-GFP fluorescence was also outside the nucleus. There was almost no co-localization of Rad23-GFP with MitoTracker (Fig. 4A).

In some cases during the co-localization experiments, Rad23-GFP appeared to be in the periphery of the nucleus. The localization was explored in the Rad23-GFP strain grown in the absence of stress or 1 h after being given a low dose of UV light (120 J/m^2). In the absence of stress Rad23-GFP was most often around the edge of the nucleus, as well as being cytoplasmic, and shifted to being within the nucleus in response to UV stress (Fig. 5). Quantification with >100 cells under each condition reveals that Rad23 is mostly located around the edge of the nucleus (cytoplasmic 14%, perinuclear 86%, nuclear 0%; n = 131) in the absence of stress, after which most cells have Rad23 within the nucleus (cytoplasmic 11%, perinuclear 2%, nuclear 86%; n = 162). The reason for the perinuclear distribution is yet to be established; however, that location is consistent with being the nuclear envelope-endoplasmic reticulum network where proteasomal components are concentrated in *S. cerevisiae* and *Schizosaccharomyces pombe* (Enenkel et al., 1998; Wilkinson et al., 1998).

The survival of animals inoculated with strains carrying different deletions in *RAD23* implicates the UBA2 domain of Rad23 being key for the virulence of *C. neoformans*. Hence, we examined the localization and protein level of this Rad23-uba2Δ isoform missing its UBA2 domain for two reasons. First, the removal of the domain might alter the localization of the protein. Second, the reduced virulence observed for strains missing the UBA2 domain may be simply a reflection of the overall stability of the protein in the absence of this domain. The *RAD23-uba2*Δ*-GFP* construct was expressed in the *rad23*Δ strain background. Microscopy revealed that the Rad23-uba2Δ-GFP expression level (Fig. 6A) was qualitatively equivalent to that of full-length Rad23-GFP strain in yeast cells (Fig. 4). We also tested the wild type, *rad23*Δ, *rad23*Δ+*RAD23-uba2*Δ, *rad23*Δ+*RAD23-uba2*Δ-GFP and *rad23*Δ+*RAD23*-GFP strains for their responses to the presence

of tunicamycin (Fig. 6B). We observed that *rad23*Δ, *rad23*Δ+*RAD23-uba2*Δ and *rad23*Δ+*RAD23-uba2*Δ-*GFP* strains showed comparable phenotypes with more growth in the presence of tunicamycin, while wild type and the full length *RAD23-GFP* complemented strain, *rad23*Δ+*RAD*23-*GFP*, had comparable phenotype in the presence of tunicamycin. Hence, the virulence defect observed for the UBA2 domain deletion strain was not because of destabilization of the protein in the absence of the degradation resistance signal but because of some other reason, most likely through impairment in the UPR.

4. Discussion

DNA repair enzymes and their "moonlighting" functions in other cellular pathways have been explored in depth in model organisms (Gancedo et al., 2016; Khan et al., 2014). However, there are differences between established model systems, such as budding and fission yeasts, with other organisms and therefore there is a need to explore gene functions more widely. Furthermore, there are genes in pathogenic species in the genera *Candida* or *Cryptococcus* for which no homologs exist in model yeasts *S. cerevisiae* or *S. pombe*, or there are functional differences amongst them and these well-established models (Verma et al., 2018). DNA repair pathways aid in survival of microbial pathogens in the environment by reversing the effects of DNA-damaging stresses. The pathways may also play a role in infected hosts, as observed for *C. neoformans*, by combating oxidative and free radical stresses, through interactions with macrophages and neutrophils, wherein directly or indirectly DNA repair pathways may be necessary for fungal virulence. Such assumptions are supported by evidence of DNA repair genes in the pathogenic fungus *C. albicans* being required for virulence (Chauhan et al., 2005) and also in factors that will impact virulence

such as phenotypic switching and genome rearrangements (Alby and Bennett, 2009; Mitra et al., 2014).

C. neoformans is an important fungal pathogen that has been developed as a model system for discovering virulence-related mechanisms in pathogenic fungi (Heitman et al., 2011; Rajasingham et al., 2017). However, to date there has been limited analysis on DNA repair mechanisms (Billmyre et al., 2017; Boyce et al., 2017; Jung et al., 2019; Jung et al., 2016; Verma and Idnurm, 2013). By examining a collection of DNA repair genes that had been mutated and were implicated in virulence in a mouse model of disease (Liu et al., 2008), the *RAD23* gene was particularly interesting because it has two functions, in DNA repair and as a ubiquitin receptor protein involved in the proteasomal degradation pathway and ERAD (Dantuma et al., 2009). Through the experiments reported here in *C. neoformans* we draw two conclusions about the role of *RAD23* in virulence. First, we are able to uncouple the role of DNA repair (at least Rad4-dependent NER function) versus ubiquitin receptor function in virulence. Second, of the four conserved domains in Rad23, we narrowed down the UBA2 domain as the most important for the virulence of *C. neoformans*. The Rad4-dependent NER function of Rad23 conferred by the XPC-binding domain plays no major role in virulence. This is further supported by evidence that *rad4* and *rad23* mutants do not have identical phenotypes. The *rad4*Δ strain is far more UV-sensitive than *rad23*Δ (supplemental figure 5 in Verma and Idnurm, 2013) and has no reduction in virulence in a mouse model (Liu et al., 2008).

We compared stress and virulence phenotypes caused by the deletion of the four Rad23 domains, individually and in combinations. The UBA2 domain stood out for a role in virulence, as strains

with the allele of *RAD23* mutated in this region had a reduction in virulence that was comparable to when the *rad23*Δ complete deletion strain was used to infect larvae. The UBA2 domain is one of two ubiquitin-binding domains in the Rad23 protein. In *S. cerevisiae* the UBA2 domain binds to ubiquitin molecules and Rad23's own UBL domain. Interaction of the UBA2 domain with the UBL domain is important for the proteasome binding function of Rad23. If there is interaction between UBL and UBA domains then Rad23 will be in closed confirmation and its interaction with the proteasome will be hampered. UBA2 is also required for the overall stability of Rad23 as UBA2 efficiently channels a substrate for degradation while preventing its own degradation by the proteasome (Heinen et al., 2011). If such is the case, then it is possible that the virulence defect we see for the UBA2 domain deletion strain is because of the destabilization the whole protein. However, expression of *RAD23-uba2*Δ*-GFP* in the *rad23*Δ strain background counters this hypothesis (Fig. 6) because deletion of the domain did not trigger degradation, although this is with a caveat that a constitutive promoter drives the expression of the GFP fusion constructs used in this study. The virulence defect observed for the Rad23 UBA2 domain deletion strain could be from a ubiquitin receptor function, which has roles in both the unfolded protein response and ubiquitin proteasome system, which in turn can affect the turnover of other proteins. Also, it is possible that the role of Rad23 in protein degradation by the proteasome is affected but not observed under normal conditions (normal GFP expression), but when given stress, such as during growth in a mammal or insect host, Rad23's turnover is affected.

Another possibility is that the lack of a proteasome initiation region allows Rad23 to escape degradation (Fishbain et al., 2011). These proteasome initiation regions are defined as unstructured loops or sequences, which can trigger degradation. Fishbain et al. showed that even in the absence

of the UBA2 domain, which according to previous reports is required for Rad23 stability, Rad23 could be protected from degradation on addition of a structured domain such as from dihydrofolate reductase (DHFR). This study suggests that it is possible that tagging the UBA2 domain truncated Rad23 with GFP at its C-terminal end might cover the unstructured region exposed due to deletion of the UBA2 domain, such that the Rad23-GFP fusion escapes degradation. If so, the scenario for the virulence defect we observe in the Rad23 UBA2 domain deletion strains might be due to instability of Rad23 and hence lack of its ubiquitin adaptor functions. However, the *rad23*Δ+*RAD23-uba2*Δ-*GFP* strain has a comparable stress phenotype as the *rad23*Δ and *rad23*Δ+*RAD23-uba2*Δ strains (Fig. 6B), suggesting that the virulence defect observed is because of the missing UBA2 domain function and is not due to an issue with Rad23 protein stability.

In *S. cerevisiae* the XPC-binding domain physically interacts with Rad4 and Png1. *C. neoformans* has a homolog for Rad4 but no homolog for Png1. An interaction of Rad4, which is a major NER protein, with this domain of Rad23 can explain the UV sensitivity phenotype seen in the strain with the XPC-binding domain deleted. However, as no homolog of Png1 exists in *C. neoformans*, the reason for the tunicamycin resistance phenotype observed for the XPC-binding domain deletion strain is unknown. A tunicamycin resistance phenotype, stronger than what is seen here for the *rad23* mutants, is observed in the *puf4* deletion strain (Glazier et al., 2015). Puf4 is a mRNA-binding protein with a role in regulating the UPR. The basis of resistance is unknown, but hypothesized to be due to altered production of Alg7, the UDP-*N*-acetylglucosamine-1-phosphate transferase that is targeted by tunicamycin (Glazier et al., 2015). The UBA2 domain of Rad23 in *S. cerevisiae* interacts with ubiquitin and its own UBL domain. In humans the UBA2 domains of the Rad23 A and B proteins bind to DNA repair protein 3-methyladenine DNA glycosylase (Miao

et al., 2000) and human Rad23 A protein's UBA2 domain binds to human immunodeficiency (HIV) 1 accessory protein Vpr (Withers-Ward et al., 2000): no homologs for these proteins exist in *C. neoformans* as assessed by BLASTp analysis of its genome sequence. Hence it is difficult to explain the slight UV sensitivity phenotype observed for the UBA2 domain deletion strain based on the protein interaction possibilities with DNA repair proteins.

Several conclusions emerge from this study. The first is that the UBA2 domain of Rad23 is the most important domain required for virulence of *C. neoformans*. The second is that XPCB deletion does not affect the virulence potential of *C. neoformans* yet does the UV sensitivity phenotype. XPCB is clearly implicated in the Rad4-dependent NER pathway in other eukaryotes, and hence these data indicate that Rad23's role in NER does not impact the virulence aspect of the *C. neoformans* homolog. This study also provides the evidence that pathways such as DNA repair, which are clearly important for genomic integrity, environmental survival, and evolution, may not be important for virulence. Though the functions of Rad23 in virulence of *C. neoformans* were successfully separated and tested, how exactly the ubiquitin receptor function of Rad23 regulates virulence remains to be explored in detail.

Acknowledgments

We thank the University of Missouri-Kansas City and the University of Melbourne for providing support for this work. A.I. was a Future Fellow of the Australian Research Council.

References

460 Alby, K., Bennett, R.J., 2009. Stress-induced phenotypic switching in *Candida albicans*. Mol.
461 Biol. Cell 20, 3178-3191.
462 Arras, S.D.M., Ormerod, K.L., Erpf, P.E., Espinosa, M.I., Carpenter, A.C., Blundell, R.D.,
463 Stowasser, S.R., Schulz, B.L., Tanurdzic, M., Fraser, J.A., 2017. Convergent
464 microevolution of *Cryptococcus neoformans* hypervirulence in the laboratory and the
465 clinic. Sci. Rep. 7, 17918.
466 Bahn, Y.-S., Jung, K.-W., 2013. Stress signaling pathways for the pathogenicity of
467 *Cryptococcus*. Eukaryot. Cell 12, 1564-1577.
468 Bertolaet, B.L., Clarke, D.J., Wolff, M., Watson, M.H., Henze, M., Divita, G., Reed, S.I., 2001.
469 UBA domains of DNA damage-inducible proteins interact with ubiquitin. Nat. Struct.
470 Biol. 8, 417-422.
471 Billmyre, R.B., Clancey, S.A., Heitman, J., 2017. Natural mismatch repair mutations mediate
472 phenotypic diversity and drug resistance in *Cryptococcus deuterogattii*. eLife 6, e28802.
473 Boyce, K.J., Wang, Y., Verma, S., Shakya, V.P.S., Xue, C., Idnurm, A., 2017. Mismatch repair
474 of DNA replication errors contributes to microevolution in the pathogenic fungus
475 *Cryptococcus neoformans*. mBio 8, e00595-17.
476 Chauhan, N., Ciudad, T., Rodríguez-Alejandre, A., Larriba, G., Calderone, R., Andaluz, E.,
477 2005. Virulence and karyotype analyses of *rad52* mutants of *Candida albicans*:
478 regeneration of a truncated chromosome of a reintegrant strain (*rad52*/*RAD52*) in the
479 host. Infect. Immun. 73, 8069-8078.
480 Cheon, S.A., Jung, K.-W., Bahn, Y.-S., Kang, H.A., 2014. The unfolded protein response (UPR)
481 pathway in *Cryptococcus*. Virulence 5, 341-350.

482 Dantuma, N.P., Heinen, C., Hoogstraten, D., 2009. The ubiquitin receptor Rad23: at the
483 crossroads of nucleotide excision repair and proteasomal degradation. DNA Repair 8,
484 449-460.
485 Elsasser, S., Gali, R.R., Schwickart, M., Larsen, C.N., Leggett, D.S., Müller, B., Feng, M.T.,
486 Tübing, F., Dittmar, G.A.G., Finley, D., 2002. Proteasome subunit Rpn1 binds ubiquitin-
487 like protein domains. Nat. Cell Biol. 4, 725-730.
488 Enenkel, C., Lehmann, A., Kloetzel, P.-M., 1998. Subcellular distribution of proteasomes
489 implicates a major location of protein degradation in the nuclear envelope-ER network in
490 yeast. EMBO J. 17, 6144-6154.
491 Farmer, L.M., Book, A.J., Lee, K.-H., Lin, Y.-L., Fu, H., Vierstra, R.D., 2010. The RAD23
492 family provides an essential connection between the 26S proteasome and ubiquitylated
493 proteins in *Arabidopsis*. Plant Cell 22, 124-142.
494 Fishbain, S., Prakash, S., Herrig, A., Elsasser, S., Matouschek, A., 2011. Rad23 escapes
495 degradation because it lacks a proteasome initiation region. Nat. Commun. 2, 192.
496 Gancedo, C., Flores, C.-L., Gancedo, J.M., 2016. The expanding landscape of moonlighting
497 proteins in yeasts. Microbiol. Mol. Biol. Rev. 80, 765-777.
498 Glazier, V.E., Kaur, J.N., Brown, N.T., Rivera, A.A., Panepinto, J.C., 2015. Puf4 regulates both
499 splicing and decay of *HXL1* mRNA encoding the unfolded protein response transcription
500 factor in *Cryptococcus neoformans*. Eukaryot. Cell 14, 385-395.
501 Guzder, S.N., Sung, P., Prakash, L., Prakash, S., 1998. Affinity of yeast nucleotide excision
502 repair factor 2, consisting of the Rad4 and Rad23 proteins, for ultraviolet damaged DNA.
503 J. Biol. Chem. 273, 31541-31546.

504 Heinen, C., Ács, K., Hoogstraten, D., Dantuma, N.P., 2011. C-terminal UBA domains protect
505 ubiquitin receptors by preventing initiation of protein degradation. Nat. Commun. 2, 191.
506 Heitman, J., Kozel, T.R., Kwon-Chung, K.J., Perfect, J.R., Casadevall, A., Eds., 2011.
507 *Cryptococcus*: From Human Pathogen to Model Yeast. American Society for
508 Microbiology Press, Washington, D.C.
509 Ishii, T., Funakoshi, M., Kobayashi, H., 2006. Yeast Pth2 is a UBL domain-binding protein that
510 participates in the ubiquitin-proteasome pathway. EMBO J. 25, 5492-5503.
511 Janbon, G., Ormerod, K.L., Paulet, D., Byrnes, E.J., 3rd, Yadav, V., Chatterjee, G., Mullapudi,
512 N., Hon, C.-C., Billmyre, R.B., Brunel, F., Bahn, Y.-S., Chen, W., Chen, Y., Chow,
513 E.W.L., Coppée, J.Y., Floyd-Averette, A., Gaillardin, C., Gerik, K.J., Goldberg, J.,
514 Gonzalez-Hilarion, S., Gujja, S., Hamlin, J.L., Hsueh, Y.-P., Ianiri, G., Jones, S., Kodira,
515 C.D., Kozubowski, L., Lam, W., Marra, M., Mesner, L.D., Mieczkowski, P.A., Moyrand,
516 F., Nielsen, K., Proux, C., Rossignol, T., Schein, J.E., Sun, S., Wollschlaeger, C., Wood,
517 I.A., Zeng, Q., Neuvéglise, C., Newlon, C.S., Perfect, J.R., Lodge, J.K., Idnurm, A.,
518 Stajich, J.E., Kronstad, J.W., Sanyal, K., Heitman, J., Fraser, J.A., Cuomo, C.A.,
519 Dietrich, F.S., 2014. Analysis of the genome and transcriptome of *Cryptococcus*
520 *neoformans* var. *grubii* reveals complex RNA expression and microevolution leading to
521 virulence attenuation. PLoS Genet. 10, e1004261.
522 Jung, K.-W., Lee, Y., Huh, E.Y., Lee, S.C., Lim, S., Bahn, Y.-S., 2019. Rad53- and Chk1-
523 dependent DNA damage response pathways cooperatively promote fungal pathogenesis
524 and modulate antifungal drug susceptibility. mBio 10, e01726-18.

525 Jung, K.-W., Yang, D.-H., Kim, M.-K., Seo, H.S., Lim, S., Bahn, Y.-S., 2016. Unraveling fungal
526 radiation resistance regulatory networks through the genome-wide transcriptome and
527 genetic analyses of *Cryptococcus neoformans*. mBio 7, e01483-16.
528 Khan, I., Chen, Y., Dong, T., Hong, X., Takeuchi, R., Mori, H., Kihara, D., 2014. Genome-scale
529 identification and characterization of moonlighting proteins. Biol. Direct 9, 30.
530 Kim, I., Mi, K., Rao, H., 2004. Multiple interactions of Rad23 suggest a mechanism for
531 ubiquitylated substrate delivery important in proteolysis. Mol. Biol. Cell 15, 3357-3365.
532 Lahari, T., Lazaro, J., Schroeder, D.F., 2017. RAD4 and RAD23/HMR contribute to *Arabidopsis*
533 UV tolerance. Genes 9, 8.
534 Lee, J.-H., Choi, J.M., Lee, C., Yi, K.J., Cho, Y., 2005. Structure of a peptide:*N*-glycanase-
535 Rad23 complex: insight into the deglycosylation for denatured glycoproteins. Proc. Natl.
536 Acad. Sci. USA 102, 9144-9149.
537 Liu, O.W., Chun, C.D., Chow, E.D., Chen, C., Madhani, H.D., Noble, S.M., 2008. Systematic
538 genetic analysis of virulence in the human fungal pathogen *Cryptococcus neoformans*.
539 Cell 135, 174-188.
540 Liu, T.-B., Xue, C., 2011. The ubiquitin-proteasome system and F-box proteins in pathogenic
541 fungi. Mycobiology 39, 243-248.
542 Liu, T.-B., Xue, C., 2014. Fbp1-mediated ubiquitin-proteasome pathway controls *Cryptococcus*
543 *neoformans* virulence by regulating fungal intracellular growth in macrophages. Infect.
544 Immun. 82, 557-568.
545 McKnight, G.L., Cardillo, T.S., Sherman, F., 1981. An extensive deletion causing
546 overproduction of yeast iso-2-cytochrome c. Cell 25, 409-419.

547 Miao, F., Bouziane, M., Dammann, R., Masutani, C., Hanaoka, F., Pfeifer, G., O'Connor, T.R.,
548 2000. 3-Methyladenine-DNA glycosylase (MPG protein) interacts with human RAD23
549 proteins. J. Biol. Chem. 275, 28433-28438.
550 Min, J.-H., Pavletich, N.P., 2007. Recognition of DNA damage by the Rad4 nucleotide excision
551 repair protein. Nature 449, 570-575.
552 Mitra, S., Gómez-Raja, J., Larriba, G., Dubey, D.D., Sanyal, K., 2014. Rad51-Rad52 mediated
553 maintenance of centromeric chromatin in *Candida albicans*. PLoS Genet. 10, e1004344.
554 Mylonakis, E., Moreno, R., El Khoury, J.B., Idnurm, A., Heitman, J., Calderwood, S.B.,
555 Ausubel, F.M., Diener, A., 2005. *Galleria mellonella* as a model system to study
556 *Cryptococcus neoformans* pathogenesis. Infect. Immun. 73, 3842-3850.
557 Nakai, K., Kanehisa, M., 1992. A knowledge base for predicting protein localization sites in
558 eukaryotic cells. Genomics 14, 897-911.
559 Nielsen, K., Cox, G.M., Wang, P., Toffaletti, D.L., Perfect, J.R., Heitman, J., 2003. Sexual cycle
560 of *Cryptococcus neoformans* var. *grubii* and virulence of congenic **a** and α isolates.
561 Infect. Immun. 71, 4831-4841.
562 Palmer, J.M., Drees, K.P., Foster, J.T., Lindner, D.L., 2018. Extreme sensitivity to ultraviolet
563 light in the fungal pathogen causing white-nose syndrome of bats. Nat. Commun. 9, 35.
564 Rajasingham, R., Smith, R.M., Park, B.J., Jarvis, J.N., Govender, N.P., Chiller, T.M., Denning,
565 D.W., Loyse, A., Boulware, D.R., 2017. Global burden of disease of HIV-associated
566 cryptococcal meningitis: an updated analysis. Lancet Infect. Dis. 17, 873-881.
567 Verma, S., Idnurm, A., 2013. The Uve1 endonuclease is regulated by the white collar complex to
568 protect *Cryptococcus neoformans* from UV damage. PLoS Genet. 9, e1003769.

569 Verma, S., Shakya, V.P.S., Idnurm, A., 2018. Exploring and exploiting the connection between
570 mitochondria and the virulence of human pathogenic fungi. Virulence 9, 426-446.
571 Wade, S.L., Auble, D.T., 2010. The Rad23 ubiquitin receptor, the proteasome and functional
572 specificity in transcriptional control. Transcription 1, 22-26.
573 Wade, S.L., Poorey, K., Bekiranov, S., Auble, D.T., 2009. The Snf1 kinase and proteasome-
574 associated Rad23 regulate UV-responsive gene expression. EMBO J. 28, 2919-2931.
575 Walters, K.J., Lech, P.J., Goh, A.M., Wang, Q., Howley, P.M., 2003. DNA-repair protein
576 hHR23a alters its protein structure upon binding proteasomal subunit S5a. Proc. Natl.
577 Acad. Sci. USA 100, 12694-12699.
578 Watkins, J.F., Sung, P., Prakash, L., Prakash, S., 1993. The *Saccharomyces cerevisiae* DNA
579 repair gene *RAD23* encodes a nuclear protein containing a ubiquitin-like domain required
580 for biological function. Mol. Cell. Biol. 13, 7757-7765.
581 Wilkinson, C.R.M., Wallace, M., Morphew, M., Perry, P., Allshire, R., Javerzat, J.-P., McIntosh,
582 J.R., Gordon, C., 1998. Localization of the 26S proteasome during mitosis and meiosis in
583 fission yeast. EMBO J. 17, 6465-6476.
584 Withers-Ward, E.S., Mueller, T.D., Chen, I.S.Y., Feigon, J., 2000. Biochemical and structural
585 analysis of the interaction between the UBA(2) domain of the DNA repair protein
586 HHR23A and HIV-1 Vpr. Biochemistry 39, 14103-14112.
587 Yokoi, M., Hanaoka, F., 2017. Two mammalian homologs of yeast Rad23, HR23A and HR23B,
588 as multifunctional proteins. Gene 597, 1-9.
589
590

Table 1

Cryptococcus neoformans strains used in this study. KN99**a** and KN99α are isogenic wild type strains (Nielsen et al., 2003).

Name	**Genotype**
KN99**a**	Wild type, *MAT***a**
KN99α	Wild type, *MAT*α
AISVCN120	*rad23*Δ::*NAT*
AISVCN218	*rad23*Δ::*NAT*::*RAD23*::*NEO*
AISVCN250	*rad23*Δ::*NAT*+*RAD23-ubl*Δ::*NEO*
AISVCN251	*rad23*Δ::*NAT*+*RAD23-uba1*Δ::*NEO*
AISVCN252	*rad23*Δ::*NAT*+*RAD23-xpcb*Δ::*NEO*
AISVCN253	*rad23*Δ::*NAT*+*RAD23-uba2*Δ::*NEO*
AISVCN254	*rad23*Δ::*NAT*+*RAD23-ubl*Δ+*uba1*Δ::*NEO*
AISVCN255	*rad23*Δ::*NAT*+*RAD23-uba1*Δ+*uba2*Δ::*NEO*
AISVCN87	*RAD23-GFP*::*NAT*
AISVCN256	*rad23Δ::NAT*+*RAD23-GFP*::*NEO*
AISVCN258	*rad23Δ::NAT*+*RAD23-uba2*Δ*-GFP*::*NEO*

595 **Figure legends**

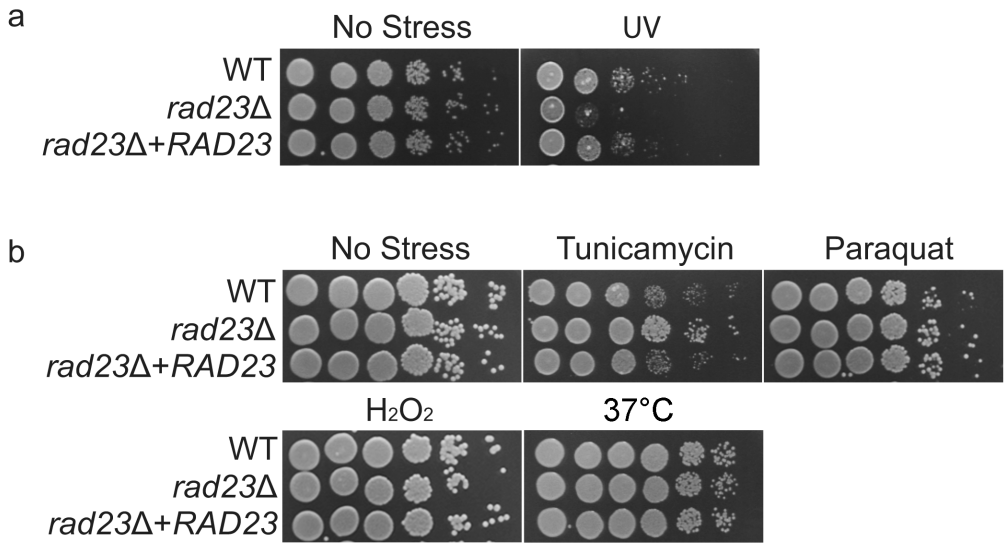

596

597 **Fig. 1.** Stress responses controlled by Rad23. The wild type (WT), *rad23*Δ and *rad23*Δ+*RAD23*

598 strains exposed to chemical, radiation and temperature stress. The stresses are tunicamycin

599 (0.125 µg/ml), hydrogen peroxide (1 mM), Paraquat (0.5 mM), 37°C and UV (120 J/m^2).

600

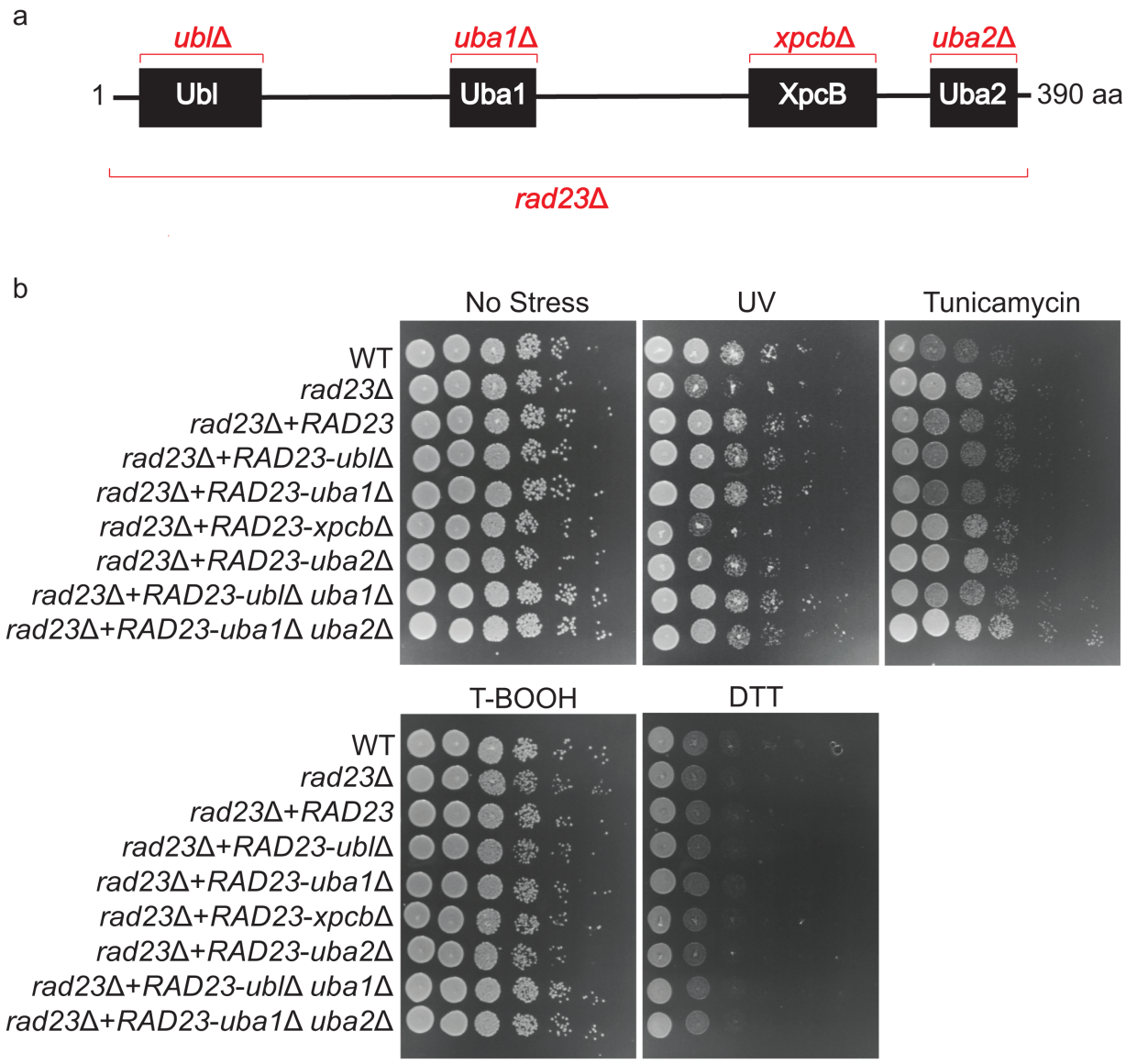

Fig. 2. Stress responses for wild type (WT) *RAD23* and variant domain deletion alleles. (A) Diagram of Rad23 representing all four domains and sites for individual domain deletions. (B) *C. neoformans* WT, *rad23*Δ and *rad23*Δ+*RAD23* complementation strain and all single and double Rad23 domain deletion strains: *rad23*Δ+*RAD23-ubl*Δ (UBL domain deletion), *rad23*Δ+*RAD23-uba1*Δ (UBA1 domain deletion), *rad23*Δ+*RAD23-xpcb*Δ (XPCB domain deletion), *rad23*Δ+*RAD23-uba2*Δ (UBA2 domain deletion), *rad23*Δ+*RAD23-ubl*Δ+*uba1*Δ (UBL+UBA1 double domain deletion) and *rad23*Δ+*RAD23-uba1*Δ+*uba2*Δ (UBA1+UBA2 double domain

609 deletion) are exposed to tunicamycin (0.125 µg/ml), DTT (10 mM), T-BOOH (0.3 mM) and UV

610 (120 J/m^2).

611

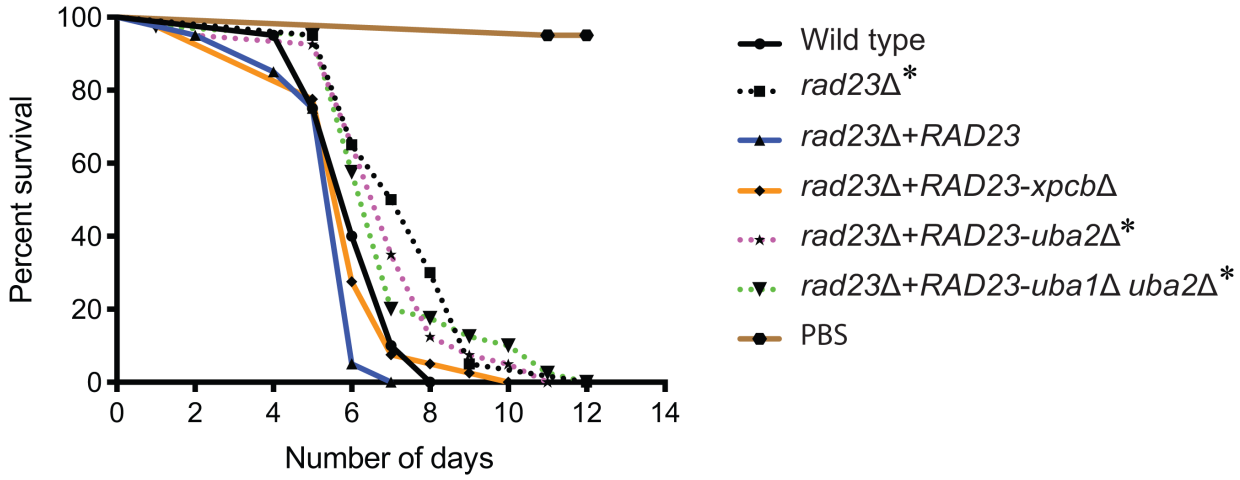

612

613 **Fig. 3.** Wax moth virulence assay for WT *RAD23* and variant domain deletion alleles. The graph

614 represents the percentage survival for wax moth larvae injected with the either PBS or 2 × 10^7

615 cells/ml of *C. neoformans*, WT (KN99**a**), *rad23*Δ and *rad23*Δ+*RAD23* strain; domain deletion

616 strains *rad23*Δ+*RAD23-xpcb*Δ (XPCB domain deletion), *rad23*Δ+*RAD23-uba2*Δ (UBA2 domain

617 deletion), *rad23*Δ+*RAD23-uba1*Δ+*uba2*Δ (UBA1+UBA2 double domain deletion) and control

618 PBS. Log-rank (Mantel-Cox) test P-values for WT versus *rad23*Δ, *rad23*Δ+*RAD23-uba2*Δ and

619 *rad23*Δ+*RAD23-uba1*Δ+*uba2*Δ strains are 0.0023 (∗), 0.0085 (∗), 0.0243 (∗), respectively. For

620 WT versus *rad23*Δ+*RAD23* strain, and *rad23*Δ+*RAD23-xpcb*Δ strain P-values were non-

621 significant (P-values > 0.05). X-axis represents percentage survival and Y-axis represents

622 number of days after infection.

623

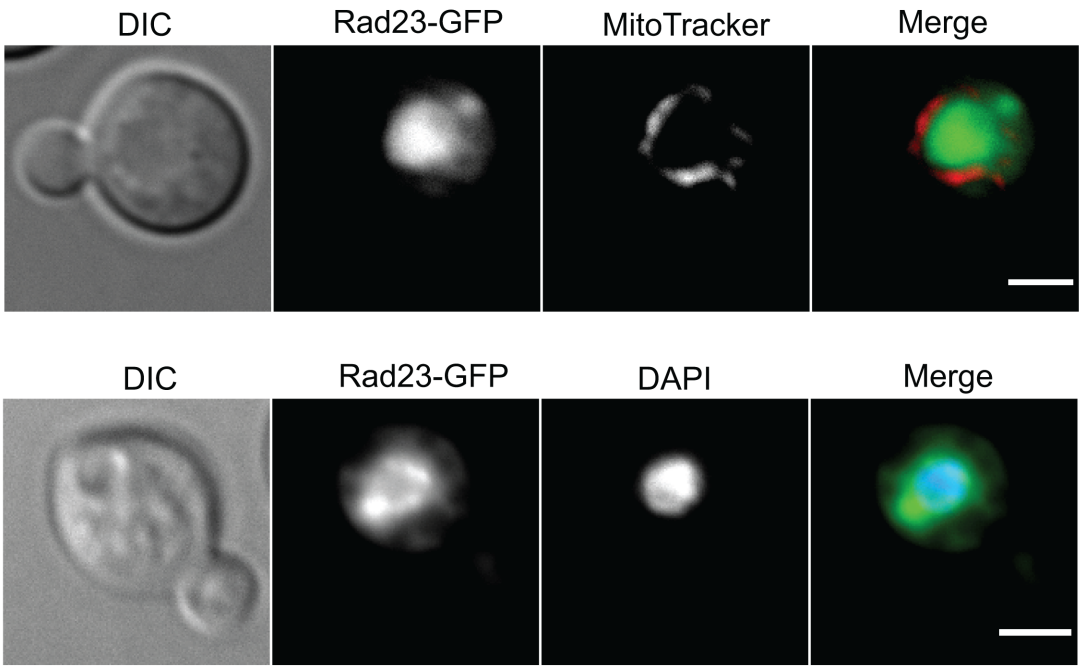

Fig. 4. Subcellular organelle localization of Rad23-GFP. Full length *RAD23-GFP* expressing strain *rad23*Δ+*RAD23-GFP* stained with mitochondrial stain MitoTracker (top panel) and nuclear stain DAPI (bottom panel). Scale bars represent 2 μm.

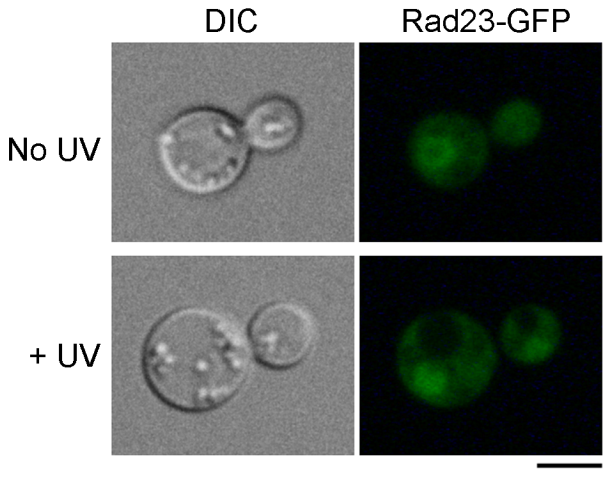

Fig. 5. Rad23 shuttles into the nucleus in response to UV stress. Cells of strain *RAD23-GFP* AISVCN87 were either cultured without UV or given a pulse of UV (120 J/m^2) and photographed 1 h later. Scale bar represents 4 μm.

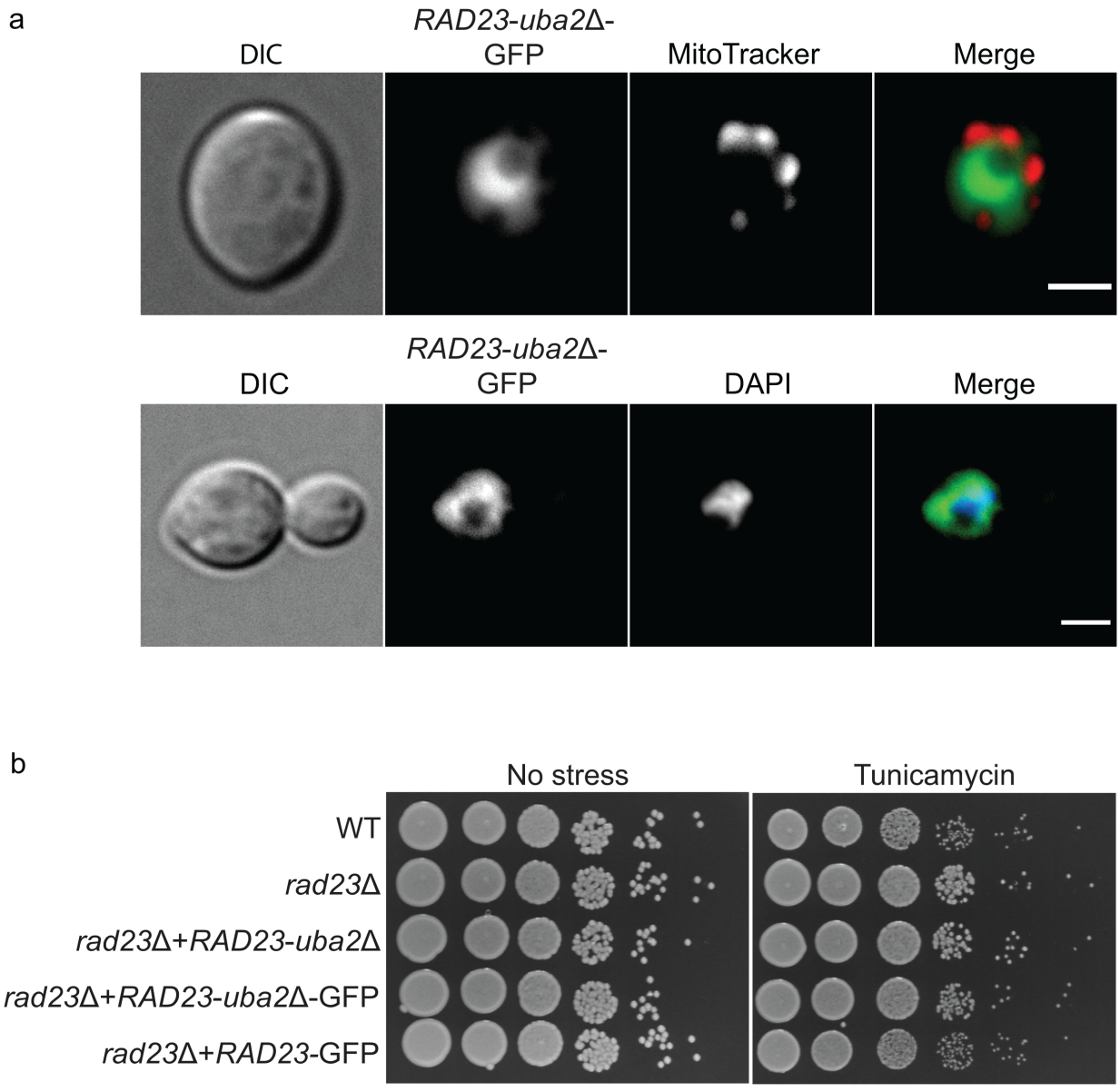

633

634 **Fig. 6.** Subcellular localization and stress phenotypes of GFP fused *RAD23-uba2*Δ. (A)

635 MitoTracker and DAPI staining for *RAD23-uba2*Δ*-GFP* expression strain in *rad23*Δ

636 background. Scale bars represents 2 µm. (B) Tunicamycin (0.125 µg/ml), stress tests for the WT,

637 *rad23*Δ, *rad23*Δ+*RAD23-uba2*Δ, *rad23*Δ+*RAD23-uba2*Δ*-GFP* and *rad23*Δ +*RAD23-GFP*

638 strains.

639

Table S1. Plasmids used in this study.

Name	Parent plasmid	Comments/Purpose
pPZP-HXK2-GFP-NATcc	(Idnurm et al., 2007)	GFP fusion by subcloning
pPZP-NEO11	(Magditch et al., 2012)	Neomycin amplification
pPZP-Pnative-*RAD23*-T-NEO	pPZP-NEO11	*RAD23* complementation construct
pPZP-Pnative-*RAD23*-UBLΔ-T-NEO	pPZP-Pnative-*RAD23*-T-NEO	Rad23 UBL domain deletion construct
pPZP-Pnative-*RAD23*-UBA1Δ-T-NEO	pPZP-Pnative-*RAD23*-T-NEO	Rad23 UBA1 domain deletion construct
pPZP-Pnative-*RAD23* XPCBΔ-T-*NEO*	pPZP-Pnative-*RAD23*-T-NEO	Rad23 XPCB domain deletion construct
pPZP-Pnative-*RAD23* UBA2Δ-T-NEO	pPZP-Pnative-*RAD23*-T-NEO	Rad23 UBA2 domain deletion construct
pPZP-Pnative-*RAD23* UBLΔ+UBA1Δ-T-NEO	pPZP-Pnative-*RAD23* DIΔ-T-NEO	Rad23 domain UBL+UBA2 deletion construct
pPZP-Pnative-*RAD23* UBA1Δ+UBA2Δ-T-NEO	pPZP-Pnative-*RAD23* DIVΔ-T-NEO	Rad23 UBA1+UBA2 domain deletion construct
pPZP-*RAD23*-GFP-NAT	pPZP-HXK2-GFP-NATcc	Rad23-GFP localization construct with NAT marker
pPZP-*RAD23*-GFP-NEO	pPZP-*RAD23*-GFP-NAT	Rad23-GFP localization construct with NEO marker
pPZP-*RAD23*-UBA2Δ-GFP-NEO	pPZP-*RAD23*-GFP-NEO	Rad23-UBA2Δ -GFP-localization construct with NEO marker

References

Idnurm, A., Giles, S.S., Perfect, J.R., Heitman, J., 2007. Peroxisome function regulates growth on glucose in the basidiomycete fungus *Cryptococcus neoformans*. Eukaryot. Cell 6, 60-72.

Magditch, D.A., Liu, T.B., Xue, C., Idnurm, A., 2012. DNA mutations mediate microevolution between host-adapted forms of the pathogenic fungus *Cryptococcus neoformans*. PLoS Pathog. 8, e1002936.

654 **Table S2.** Primers used in this study.
655

Name	Sequence 5′-3′	Template DNA	Comments
AISV149	CGAAATGAATGATCTAGGTC	D288/ H99	*rad23Δ*
AISV150	CAATTTGGCTGTCGTCCATC	D288/ H99	*rad23Δ*
AISV118	CGGGATCCCTCTGCATGATAATGTCAGCG	KN99α	*rad23*Δ complementation by *RAD23*
AISV119	CGGGATCCCGAAAGTTGGGAAAAGGGAG	KN99α	*rad23*Δ complementation by *RAD23*
AISV140	ACTGTCCAGAACAAGCCCAAAGCTACCCCTGCG	pPZP-Pnative-*RAD23*-T-NEO	*RAD23-ubl*Δ
AISV141	CGCAGGGGTAGCTTTGGGCTTGTTCTGGACAGT	pPZP-Pnative-*RAD23*-T-NEO	*RAD23-ubl*Δ
AISV142	CCTGCCTTGCAAGCTGCCGGCAACATTCCTTCTGTT	pPZP-Pnative-*RAD23*-T-NEO	*RAD23-uba1*Δ
AISV143	AACAGAAGGAATGTTGCCGGCAGCTTGCAAGGCAGG	pPZP-Pnative-*RAD23*-T-NEO	*RAD23-uba*1Δ
AISV144	GGTATGCCCGGCGGTATGGGTGGTGGTGGTGAAGGT	pPZP-Pnative-*RAD23*-T-NEO	*RAD23-xpcb*Δ
AISV145	ACCTTCACCACCACCACCCATACCGCCGGGCATACC	pPZP-Pnative-*RAD23*-T-NEO	*RAD23-xpcb*Δ
AISV146	GTGAATCTGACACAGGAGCTGTTTGAGAACATGGAG	pPZP-Pnative-*RAD23*-T-NEO	*RAD23-uba*2Δ
AISV147	CTCCATGTTCTCAAACAGCTCCTGTGTCAGATTCAC	pPZP-Pnative-*RAD23*-T-NEO	*RAD23-uba*2Δ
AISV165	CATGCCATGGTCAAGATCACTTTC	KN99α	*RAD23* GFP localization
AISV166	CATGCCATGGGTTGATCCTCCTCCATG	KN99α	*RAD23* GFP localization

656